

## Deuteron NMR methods for studying molecular order and motion in solid polymers and liquid crystalline polymers

H. W. Spiess

Max-Planck-Institut für Polymerforschung, Postfach 3148, D-6500 Mainz, FRG.

**Abstract** - Pulsed deuteron NMR offers unique possibilities for studying molecular order and dynamics in polymers exhibiting non-crystalline order. From the analysis of deuteron NMR spectra the complete orientational distribution function for individual structural elements can be determined. By analysing the line shapes of  $^2\text{H}$  absorption-, solid echo- and spin alignment spectra both type and timescale of rotational motions can be determined over an extraordinary wide range of characteristic frequencies, approximately 10 MHz to 0.01 Hz. In addition, the spin lattice relaxation of the deuterons can be exploited to extend the dynamic range to faster motions up to 10 GHz, to detect motions which do not change the NMR spectra, and to characterize the heterogeneous nature of the molecular dynamics in glassy polymers.

The techniques are illustrated by experimental examples including the characterization of the ultraslow small angle reorientation of chain segments of polystyrene in the vicinity of the glass transition and the direct determination of the distribution of correlation times for local motions in polycarbonate. In thermotropic side chain liquid crystalline polymers largely different order of the mesogenic group, spacer and main chain is detected. In the glassy state significant motional heterogeneity is observed for the mesogenic groups despite of their high orientational order. In polymer model membranes, which form lyotropic liquid crystalline phases, vastly different mobility is detected for different structural elements. Well above the phase transition the groups close to the polymer chain are blocked, whereas the mobility of the lipid chains is almost as high as in the corresponding monomer membranes.

### INTRODUCTION

The detailed characterization of molecular order and mobility should provide the basis for the understanding of the macroscopic behaviour of materials on a molecular level. As far as solid or solid-like materials are concerned molecular order can fully be characterized in principle by scattering techniques. Although they were originally restricted to crystalline solids, methods have been developed to extend the applicability of, e.g., x-ray diffraction to non-crystalline polymers (refs. 1-3). Quasi-elastic scattering, in particular of neutrons, should provide a detailed description of rotational and translational motions in polymers (refs. 4-5). The slow or ultraslow motions in solid polymers, however, are far beyond the resolution currently available, even by the neutron spin-echo technique (ref. 6).

Besides scattering, a number of spectroscopic techniques are available that are able to characterize molecular order and mobility in solid polymers (refs. 7-10, for recent reviews cf. refs. 11, 12). Most methods, however, yield rather crude information only, through order parameters and correlation times based on observables depending on low powers of angular functions involving molecular orientation, e.g. Legendre polynomials  $P_1(\cos \theta)$  with  $0 \leq l \leq 4$ ,  $\theta$  being the angle between a molecular axis and a selected direction of the sample or of an external field. Pulsed deuteron NMR, on the other hand, yields much more precise information, because the NMR frequency itself depends on molecular orientation:

$$\omega = \omega_0 \pm \delta (3 \cos^2 \theta - 1 - \eta \sin^2 \theta \cos 2\phi) = \omega_0 \pm \omega_Q \quad (1)$$

due to the quadrupole interaction of the deuteron spin  $I = 1$  and the electric field gradient at the deuteron site (ref. 13). Here  $\delta$  is  $3/8$  times the quadrupole coupling constant  $e^2qQ/\hbar$ ,  $\eta$  is the asymmetry parameter ( $0 \leq \eta \leq 1$ ) and the polar angles  $\theta$  and  $\phi$  specify

the orientation of the magnetic field in the principal axes system of the electric field gradient tensor (FGT). For deuterons in C-H bonds, the field gradient is essentially axially symmetric about that bond direction ( $\eta \approx 0$ ) and therefore the quadrupole frequency, again, is proportional to  $P_2(\cos \theta)$  only. Note, however, that in highly resolved spectra frequencies can be measured very accurately. This becomes clear if we look at the primary information, i.e. the NMR signal in the time domain:

$$G(t) \propto \exp(i\omega_Q t) \quad (2)$$

which depends - through expansion of the exponential - on extremely high even powers of  $\cos \theta$ , limited by the spectral resolution only. Moreover, as will be shown below the NMR-signals at even vastly different times can directly be correlated, giving detailed information about the dynamic processes. Therefore,  $^2\text{H}$  NMR offers unique possibilities for the characterization of molecular dynamics and order in polymers (for reviews cf. refs. 14-16). The main advantages of pulsed deuteron NMR can be summarized as follows:

Deuterons represent well-defined nuclear spin labels since they monitor the orientation of individual C-H bond directions, see above.

Different motional mechanisms can clearly be distinguished because they lead to often vastly different NMR spectral line shapes.

The dynamic range over which polymer mobility can be followed is extremely high ( $10^{10}$  Hz -  $10^{-2}$  Hz).

Motional heterogeneity can be detected in non-crystalline polymers.

Deuteron NMR is highly selective, because order and mobility of different groups of the monomer unit can be studied separately, in particular through selective isotopic labelling.

Deuteron NMR line shapes provide detailed information about molecular order, i.e. the complete orientational distribution function.

In the following section the techniques for studying molecular motions and order will briefly be introduced. The experimental examples provided in the subsequent sections concentrate on the nature of the chain motions associated with the glass-transition, on the determination of the distribution of correlation times for local motions in glassy polymers, the different degrees of order and mobility of the individual functional groups in liquid crystalline polymers and the different degrees of motional hindrance at the individual segments of a polymer model membrane.

## TECHNIQUES

The use of pulsed deuteron NMR for studying molecular motions and the different time scales involved are best discussed in connection with the Jeener-Broekaert three-pulse sequence (ref. 17), depicted for convenience in Fig. 1.

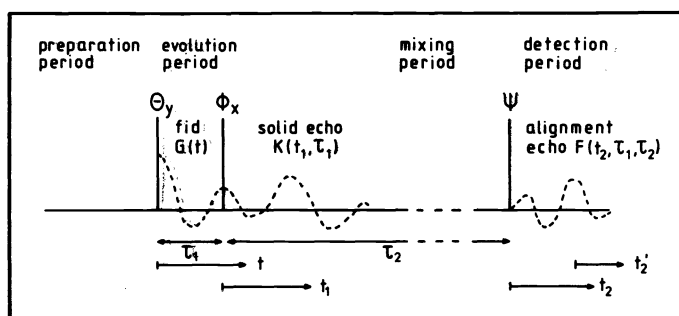


Fig. 1. The generalized Jeener Broekaert three-pulse sequence (ref. 17) and the NMR signals following the various pulses.

Fourier transform (FT) of the free induction decay (FID),  $G(t)$  following a single pulse yields, in principle, the true absorption spectrum. The large spectral width of the solid state spectra, typically 250 kHz, cf. refs. 14-16, generates problems, because considerable information is lost during the inevitable dead time of the receiver. This problem can be overcome by generating a solid echo ( $\phi_x = \pi/2$ ) and taking the FT starting at the echo maximum.

In presence of motion, however, refocussing by the second pulse will be incomplete and the solid echo decays with increasing  $\tau_1$ . Moreover the line shapes obtained through FT of the solid-echo signal are affected by the motion (ref. 18). Since different motions involve different changes of the orientation of the labelled C-H bond directions they lead to different NMR line shapes. The evolution time  $\tau_1$  can typically be varied between 15  $\mu\text{s}$  and 200  $\mu\text{s}$ . As a consequence, the solid-echo technique is able to monitor slow rotational motions with correlation times between  $10^{-4}$ s and  $10^{-7}$ s (for details see refs. 14, 16, 18).

The solid echo technique is limited by the transverse relaxation of the deuterons, resulting in particular from the dipolar interaction of the deuterons with neighbouring spins. It is characterized by a time constant  $T_2^* \lesssim 200$  s. Ultraslow motions with correlation times exceeding  $T_2^*$  significantly thus cannot be studied by solid-echo spectroscopy. The spin alignment technique (ref. 19), however, circumvents transverse relaxation and is limited by longitudinal relaxation only. Since the corresponding time constant  $T_1$  in solids can exceed 100s, ultraslow motions with correlation times between  $10^{-4}$ s and 100s can be studied this way. Spin alignment, created by choosing  $\phi_x = \pi/4$  is a long lived state of order of the deuteron spin system, where the spins are aligned parallel and antiparallel to the external magnetic field. After a waiting- or mixing time  $\tau_2$  a reading pulse  $\psi = \pi/4$  generates an alignment echo, cf. Fig. 1. This NMR signal is directly proportional to a single particle correlation function:

$$F(t_2, \tau_1, \tau_2) = \langle \sin[\omega_Q(0)\tau_1] \cdot \sin[\omega_Q(\tau_2)t_2] \rangle \quad (3)$$

depending on the values of  $\omega_Q$  and thus on the molecular orientation in the evolution period  $t = 0$  and the detection period  $t = \tau_2$ , respectively, for details cf. ref. 19. Ultraslow molecular motions on the rather long time scale  $\tau_2$  lead to a reduction of the alignment echo intensity and characteristic spectral changes in the spin alignment spectra generated by FT of the alignment echo signal.

Faster motions on the other hand, with correlation times between  $10^{-7}$ s and  $10^{-10}$ s can also be studied by analysing the frequency dependent spin lattice relaxation, in particular of spin alignment. This again leads to characteristic line shape changes which can be analysed to yield information about the type as well as the time scale of molecular motions. Moreover, since the spin lattice relaxation depends on spectral densities which have angular dependences different from that of the NMR frequency, motional features can be detected that do not affect the NMR spectrum itself (ref. 20).

### CHAIN MOTION AT THE GLASS TRANSITION

Deuteron spin alignment is particularly suited to characterize the ultraslow chain motions associated with the glass transition. It can detect motions which change the NMR frequency during the rather long mixing time  $\tau_2$ , which typically is in the range  $\mu\text{s} - 10\text{s}$ . The onset of chain motion above the glass transition temperature  $T_g$  first of all manifests itself in a rapid decay of the alignment echo (refs. 16, 21). The time constant of the initial decay strongly depends on the evolution time  $\tau_1$ . This indicates diffusive motion by small but not well-defined angles. In close proximity to  $T_g$  this diffusive motion is extremely slow, involving small angle rotations only, even after long times. This is illustrated in Figs. 2 and 3, where experimental and calculated spin alignment spectra are plotted for polystyrene (ref. 22). Note that the FT is taken with zero time delay after the third pulse. This is achieved adding a refocussing pulse in the detection period (refs. 22, 23). For  $\tau_1 = 17 \mu\text{s}$  the alignment echo has decayed far below 10% of its initial value for the mixing times 2s and 0.2s at 378 K and 388 K, respectively, cf. also the corresponding curves plotted in Fig. 19 of ref. 16. Nevertheless at 378 K the line shape changes associated

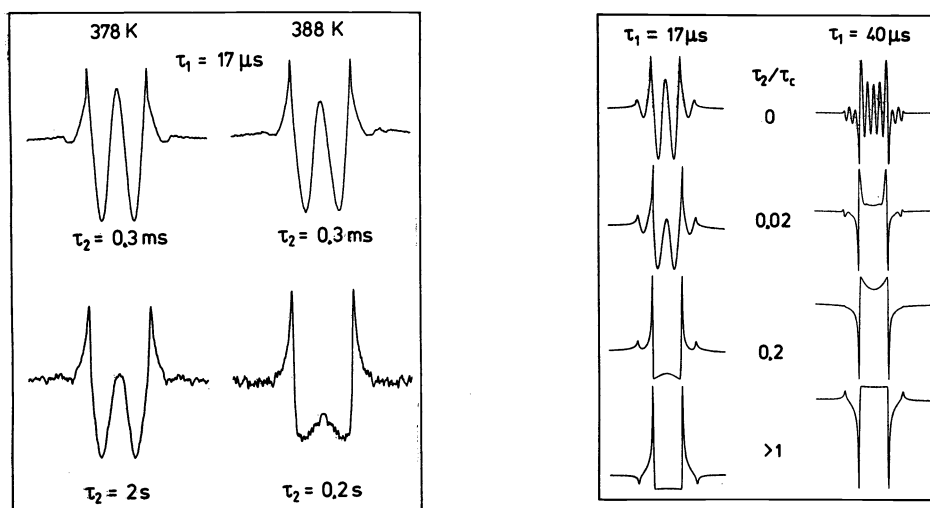


Fig. 3. Calculated  $^2\text{H}$  spin alignment spectra for different evolution times  $\tau_1$  and different ratios of the mixing time  $\tau_2$  and the correlation times  $\tau_c$ .

Fig. 2.  $^2\text{H}$  spin alignment spectra of chain deuterated polystyrene above  $T_g$

with this decay are rather minor. At 388 K, on the other hand, not only does the decay of the alignment echo occur on a much shorter time scale, but also is associated with a major change in the line shape. In Fig. 3 theoretical line shapes are plotted, calculated for diffusive motion. Note in particular that major changes in the spin alignment spectra occur for mixing times  $\tau_2$  well below the correlation time  $\tau_c$ , in particular for long evolution times  $\tau_1$ . The spectra are strongly dependent on  $\tau_1$  for  $\tau_2/\tau_c \ll 1$  but become independent of  $\tau_1$  for long mixing times  $\tau_2/\tau_c > 1$ , apart from the sign. Long mixing times  $\tau_2$  correspond to complete randomization of the molecular orientation, whereas at  $\tau_2/\tau_c \ll 1$  small angle rotations are possible only. The experimental spectra can be fitted by the line shapes calculated for diffusive motion, cf. Figs. 2 and 3 and from the fit it can be inferred that at 378 K each chain segment after 2s has rotated by approximately  $\pm 4^\circ$  only, whereas at 388 K after 0.2s it has rotated by approximately  $\pm 15^\circ$  already. Thus deuteron spin alignment is able to give a detailed characterization of ultraslow motions, even if they are highly restricted and involve rotations by a few degrees only, (see above). Our experiments thus allow us to follow the increasing cooperativity of the chain motion with increasing temperature by specifying the angular region a given C-H bond direction can explore within a given time, details will be published at a later date (ref. 22).

## DISTRIBUTIONS OF CORRELATION TIMES

The correlation functions of dynamic processes in glassy polymers typically exhibit non-exponential decays. This is known from dielectric and mechanical relaxation studies as well as from photon correlation spectroscopy and NMR relaxation measurements (refs. 24-27). It is customary to analyse experimental data in terms of a distribution of correlation times. Little is known, however, about the nature of this distribution. In particular, most techniques employed in this area do not allow to distinguish between a heterogeneous distribution, where spatially separated groups move with different time constants, and a homogeneous distribution, where each monomer unit exhibits essentially the same non-exponential relaxation. Even worse, relaxation processes resulting from different motional mechanisms often cannot be separated. Thus, if different motions have adjacent or even overlapping distributions of correlation times unselective experiments may easily be misinterpreted to indicate extremely broad distributions.

Pulsed deuteron NMR offers new possibilities in this area (refs. 16, 28). This holds in particular, if the distribution of correlation times covers the "intermediate exchange region", i.e.  $10^{-7}\text{s} < \tau_c \leq 10^{-4}\text{s}$ . Then the distribution of  $\tau_c$  manifests itself in three observables, line shape as a function of  $\tau_1$ , spectral intensity as a function of  $\tau_1$  and non-exponential spin-lattice relaxation. As an example in Fig. 4 a log-Gaussian distribution of correlation frequencies  $\Omega \propto \tau_c^{-1}$ , the intensity of the solid echo spectra as a function of  $\ln \Omega$  and spectra for selected values of  $\Omega$  are plotted for the three-site-jump of methyl groups (ref. 28). The total spectrum is a weighted superposition of the individual line shapes, as shown in Fig. 5, where experimental and calculated spectra of the methyl deuterons of polycarbonate (PC) are plotted for different temperatures and different evolution times. Note that all essential features of the experimental spectra are reproduced by the fitted calculated line shapes, based on a log-Gaussian distribution 2.3 decades in width.

By combination with spin-lattice relaxation experiments we can prove the heterogeneous nature of the distribution, because it leads to non-exponential relaxation of the deuteron spin magnetization as shown in Fig. 6. The line shapes for partially and fully relaxed spectra differ markedly as also shown in Fig. 6. Here  $\tau_0$  denotes the time the deuterons are allowed to relax after a saturation sequence before the spectra are taken via the solid echo technique. Line shape changes are observed for  $\tau_0$  being as long as several seconds, whereas the center of the distribution of correlation times is  $\tau_{c0} = 3 \cdot 10^{-6}\text{s}$ . This means that slower and faster rotating methyl groups moving with correlation times between  $10^{-5}\text{s}$  and  $10^{-7}\text{s}$ , respectively, do not change their motional behaviour on a time scale of at least a second and, therefore, must be spatially separated.

The distribution of correlation times probably arises from differences in packing at the different sites in the amorphous phase. Slight differences in the activation energy  $E_a$  for local motions - between 15 and 21 kJ/mol in our particular case - lead to considerable distributions of correlation times. Our current investigations of the interrelation between the macroscopic behaviour of polymers and their molecular dynamics suggest that motional heterogeneity strongly influences the mechanical properties. It is of vital importance, however, to work selectively in this area, since not all motions will couple to mechanical deformations. Likewise, in mixtures of polymers and low molecular mass additives which change the mechanical behaviour (ref. 29) typically not all of the local motions will be affected. This is demonstrated here for PC and mixtures of PC with polychlorinated biphenyls. In Fig. 7 we plot the distribution of correlation times for both methyl- and phenylene motions at the same temperature. The width of the distributions for both groups are similar and rather narrow (2.3 and 4.3 orders of magnitude, respectively). The additives leave the methyl mobility essentially unchanged, but strongly hinder the phenylene mobility, increasing drastically the width of the distribution of correlation times. Our selective experiments thus strongly suggest a relation between the phenylene mobility and the mechanical properties in this system (ref. 29).

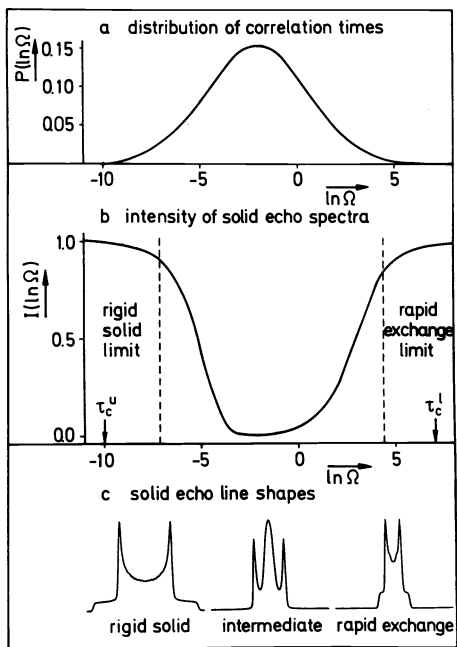


Fig. 4. Scheme for the calculation of spectra for a distribution of correlation times.

Fig. 7. Distribution of correlation frequencies for the methyl and phenylene groups in PC (solid lines) and mixtures of PC and 25% polychlorinated biphenyls (dotted lines).

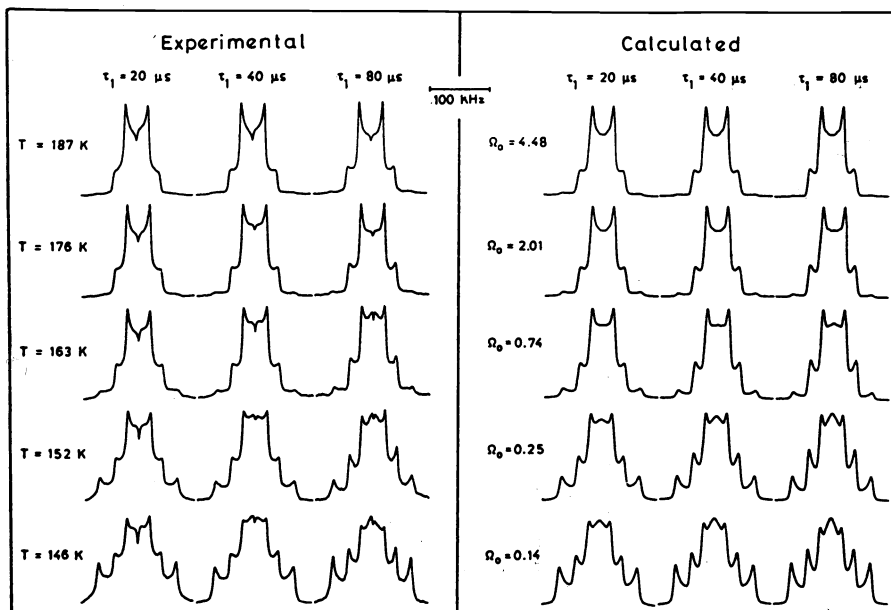
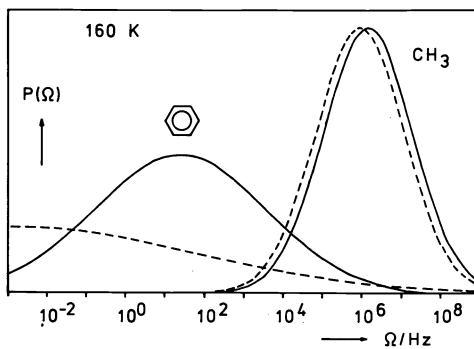


Fig. 5. Experimental and calculated methyl deuteron spectra of polycarbonate for different temperatures and different evolution times (ref. 28).

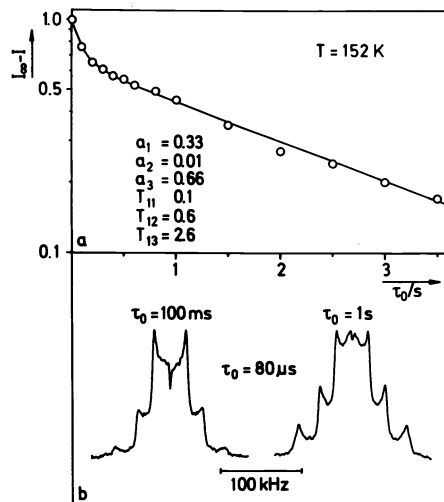


Fig. 6. Non-exponential spin-lattice relaxation and corresponding partially relaxed <sup>2</sup>H spectra for methyl deuterons in polycarbonate, for details see ref. 28.

## THERMOTROPIC LIQUID CRYSTALLINE POLYMERS

Thermotropic liquid crystalline polymers have been the subject of pure and applied research in recent years (refs. 30, 31). These polymers are usually classified into two groups, main chain and side chain polymers. The introduction of mesogenic units (rod-like or disc-shaped) in the polymer chain leads to liquid crystalline main chain polymers, the attachment as a side group results in liquid crystalline side chain polymers. The synthesis of both types is carried out using the spacer concept (ref. 32, 33), shown schematically in Fig. 8. The opposite tendencies of high molecular order for the mesogenic groups and random coils for polymers suggest a model, where the flexible spacer is introduced in order to minimize their mutual interaction. For a comprehensive understanding of the relation between structure and properties detailed investigations on chain conformation, arrangements of the mesogenic groups as well as order and mobility of both the main chains and the side groups are necessary.  $^2\text{H}$  NMR is ideally suited for such studies since the mesogenic groups, the spacers and the main chains can be investigated separately. Moreover, the molecular order in the polymers can be compared with low molecular weight analogues.

The molecular structure of the systems study is shown in Fig. 9. The phase transition temperatures were determined by DSC:  $k$  and  $g$  denote melting point and glass transition, respectively;  $s$ ,  $n$ ,  $i$  denote the transition to the liquid crystalline smectic-A, nematic phase or to the isotropic melt. Let us consider the molecular order first. In the nematic phase of the smectic system the order parameters  $S$  for the mesogenic units are strongly temperature dependent, in particular in the low molecular weight analogue (ref. 34). In the polymers, the nematic range is much wider and correspondingly the temperature dependence of  $S$  is much smaller. The order parameter for the methylene groups of the spacer and for the equivalent position of the alkyl chain of the low molecular weight analogue show a similar behaviour. In addition, however, the absolute value of  $S$  is substantially

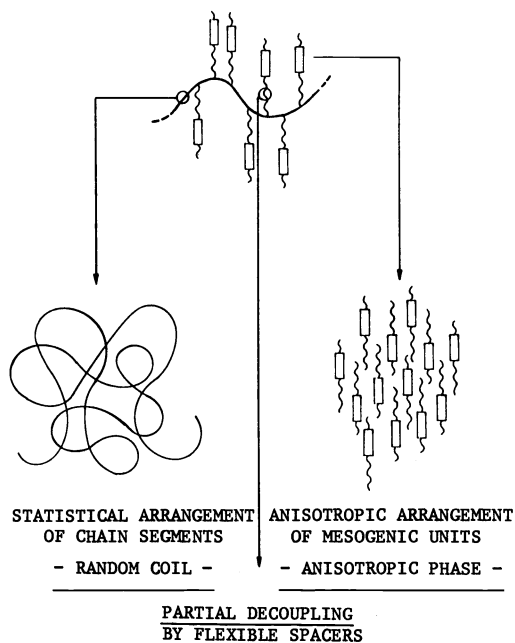


Fig. 8. Schematic structure of liquid crystalline side chain polymers, illustrating the spacer concept.

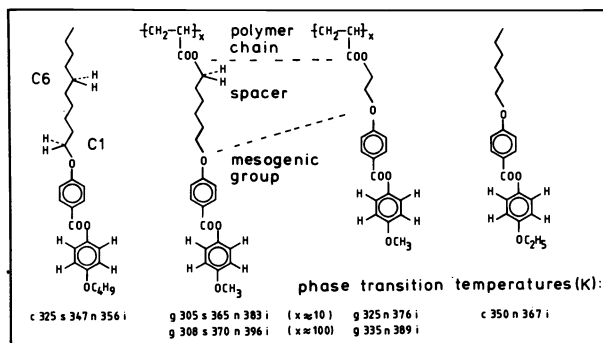


Fig. 9. Molecular structure and phase transitions of selectively deuterated liquid crystalline side chain polymer and their low molecular weight analogues.

reduced, indicating a much higher fraction of gauche conformers in the spacer of the polymer, namely 50%, for details see ref. 34. Since the labelled position of the spacer is adjacent to the main chain, a rather low order of the chain can be anticipated.

This is borne out, if the liquid crystalline polymers are cooled down into the glassy state. The order parameter of the mesogenic unit, as obtained from the angular dependence of the line shape is  $S = 0.85 \pm 0.05$  in the frozen smectic and  $S = 0.65 \pm 0.05$  in the frozen nematic, respectively (refs. 34, 35). A substantial amount of this molecular order, generated by the external magnetic field is transferred to the spacer, very little order, however, is observed for the main chain (cf. Fig. 28 of ref. 16). In Fig. 10 observed and calculated NMR spectra are plotted for the main chain deuterons in the frozen smectic polyacrylate (Fig. 9) and an analogous polymethacrylate with a spacer of 6 methylene groups, frozen from its nematic phase. Spectra are shown with director  $\vec{n}$  parallel and perpendicular to the magnetic field, respectively. The angular dependence of these spectra is rather small,

but opposite in nature for both systems. From the preliminary fitted line shapes we obtain order parameters  $S \cong +0.2$  for the polyacrylate and  $S \cong -0.3$  for the polymethacrylate. The low absolute values of the order parameter suggest that the main chain conformation can be described by a distorted random coil. In the polyacrylate the long axis of the prolate spheroid, in the polymethacrylate the short axis of the oblate spheroid is parallel to the director. For the latter the chain conformation has directly been determined by neutron scattering (ref. 36), showing that indeed perpendicular to the director the radius of gyration is about 30% larger than parallel to the director. Thus the results of neutron scattering and deuteron NMR are in good agreement. Details will be published at a later date.

The molecular motion of the mesogenic units in the glassy state was also investigated. In Fig. 11 observed and calculated  $^2\text{H}$  NMR spectra are plotted for the frozen smectic polyacrylate. Note that pronounced line shape and intensity changes are observed at temperatures far below  $T_g = 308$  K. The motional mechanism involves rotational jumps of the labelled phenylene rings by  $180^\circ$  (ref. 35). Remarkably the molecular motion cannot be described by a single correlation time. Heterogeneous mobility, characteristic of amorphous polymers, see above, is also observed here in these highly ordered glassy systems. Both, line shapes and intensities are remarkably well reproduced, Fig. 11, by a symmetric log-Gaussian distribution of correlation times, 2.6 decades in width. The corresponding semi-logarithmic plots of the distributions are presented in Fig. 12, solid lines: spacer with 6, dotted lines: spacer with 2 methylene units, respectively. The widths of the distributions are indicated

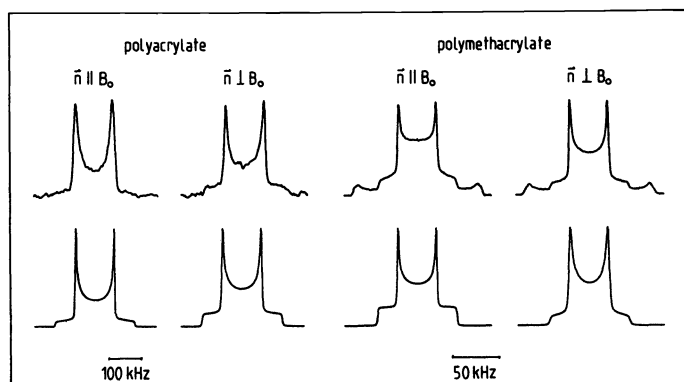


Fig. 10. Observed and calculated  $^2\text{H}$  NMR spectra of a chain deuterated liquid crystalline side chain polyacrylate and an analogous polymethacrylate.

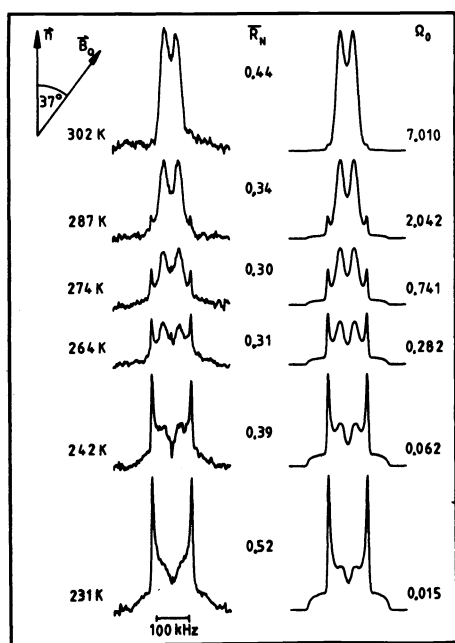


Fig. 11. Observed and calculated  $^2\text{H}$  NMR spectra for the frozen smectic polyacrylate labelled at the phenylene ring (Fig. 9).

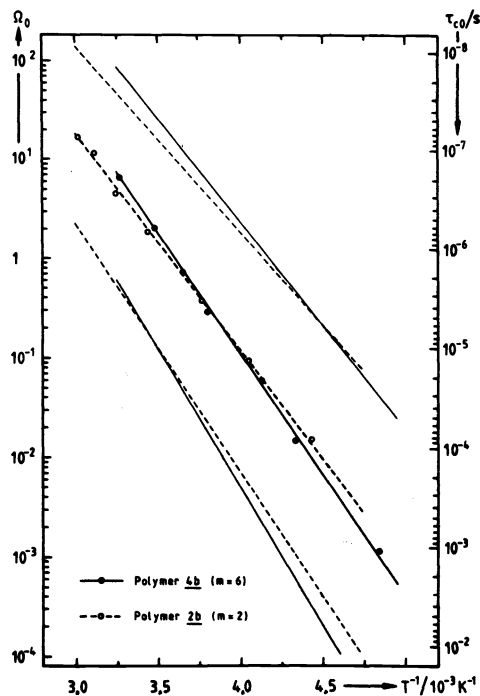


Fig. 12. Jump frequencies and correlation times for the phenylene motion in frozen liquid crystalline side chain polymers.

by the lines shifted to longer and shorter values of the correlation time. The activation energies for both systems are almost identical,  $E_a = 47 \pm 3$  and  $E_a = 42 \pm 3$  kJ/mol (ref.37). These results are in excellent agreement with those obtained from dielectric relaxation studies of the same system (ref. 38).

In summary the results of our  $^2\text{H}$  NMR investigation, in particular the study of molecular order, illustrate that the structure of such liquid crystalline side chain polymers is in accord with the predictions of the spacer model. In the glassy state, where the motion of the main chain is frozen, the side groups are not frozen in completely but exhibit local mobility similar to that observed in non-ordered glassy polymers. These frozen nematic or smectic systems thus show a high degree of non-crystalline orientational order but behave like unordered amorphous materials as far as their local dynamics is concerned.

## POLYMER MODEL MEMBRANES

Model membranes composed of simple lipid analogues easily organise themselves to form liposomes, hexagonal or lamellar phases. The stability of such systems can be substantially increased by introducing a polymerizable group and subsequent polymerization as shown in Fig. 13. Several concepts, where the polymerization is achieved either in the hydrophobic or in the hydrophylic region have been realized (ref. 39). The stabilization is always accompanied by restrictions on the mobility of the membrane, which limits its applicability.  $^2\text{H}$  NMR of selectively deuterated systems again is ideally suited to study changes in mobility that occur as a consequence of the polymerization.

Lipid analogues as well as natural lipids undergo a phase transition from a relatively ordered lamellar gel phase  $L_\beta$  to the liquid crystalline  $L_\alpha$  phase. As illustrated in Fig. 14 the phase transition temperature  $T_m$  as detected by DSC is lowered on polymerization in our system, cf. Fig. 13. Since the liquid crystalline phase is indispensable for the function of membranes, the molecular mobility in this phase is of particular interest. In Fig. 15 deuterium NMR spectra for selectively labelled positions are plotted for temperatures above and below the phase transition (ref. 40, 41) for the monomer as well as the polymer, cf. also Fig. 13. In the liquid crystalline phase of the monomer model membrane the lipid analogues have many degrees of motional freedom: conformational changes, rotation about the long axis and tilt motion of whole domains. The narrow spectra indicate that the mobility at the different positions of the molecule is very similar. In the polymer membrane, on the other hand, the line shapes differ markedly for the individual positions reflecting major differences in mobility. For a qualitative interpretation of such spectra it is important to note that the total width reflects the degree of motional freedom, the details of the line shape depend on the time scale of the motion. From Fig. 15 it is clear that the mobility of the spacer adjacent to the polymer chain is almost completely hindered, whereas in the middle of the lipid chain, at the 7-position, it is almost unchanged.

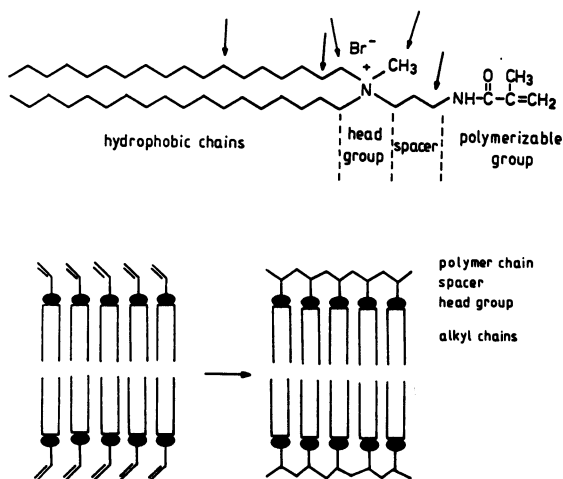


Fig. 13. Molecular structure and scheme of polymerization of the selectively deuterated polymer model membrane.

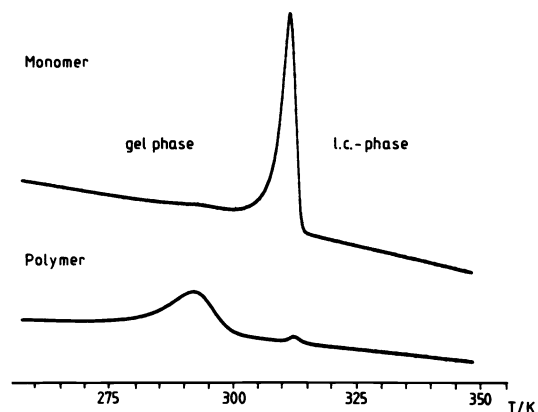


Fig. 14. Endothermic DSC diagram of the monomer and the polymer model membrane.



The NMR spectra can quantitatively be analyzed by describing the complex molecular mobility by a simple 6-site jump model (ref. 41) taking into account the conformational changes and the axial rotation. As shown in Fig. 16 the calculated line shapes are in excellent agreement with the experimental spectra, and can quantitatively describe the spectral changes resulting from varying the evolution time  $\tau_1$ , cf. Fig. 1. The increasing mobility with increasing temperature is only in part due to an increase of the jump rate  $\Omega$  between different sites. It also results from the increasing number of sites a given C-H bond direction can take on as a consequence of the motion. Thus the populations  $P$  of the various sites also change. Because of microscopic reversibility, however, the mobility of a given temperature can still be characterized by a mean jump frequency  $\bar{\Omega}$  defined by the product of  $\Omega$  and  $P$ , for details see ref. 41.

This mean jump frequency is plotted in Fig. 17 for the various positions of the monomer and the polymer membrane. In order to make the data comparable, the values of the monomer are shifted in temperature to account for the differences in the phase transition temperature  $T_m$ , cf. Fig. 14. As noted above the mean jump frequencies for the various positions of the monomer are almost alike. For the polymer major differences are observed for the

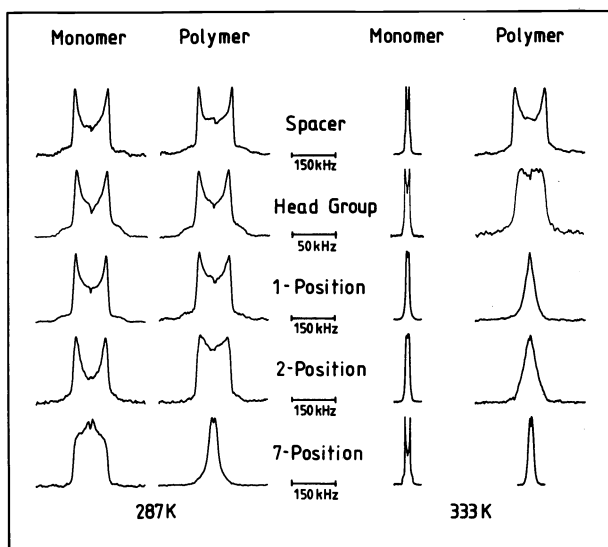


Fig. 15. Deuteron NMR spectra of the selectively deuterated monomer and polymer model membrane.

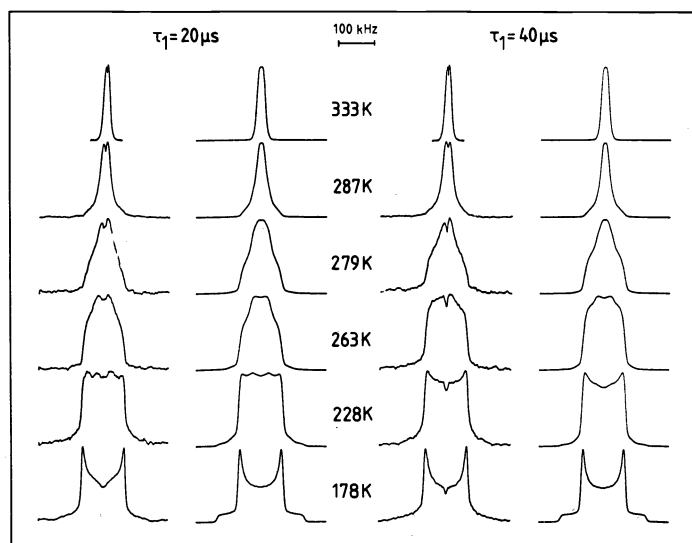


Fig. 16. Observed and calculated deuteron NMR spectra for the 7-position of the polymer model membrane.

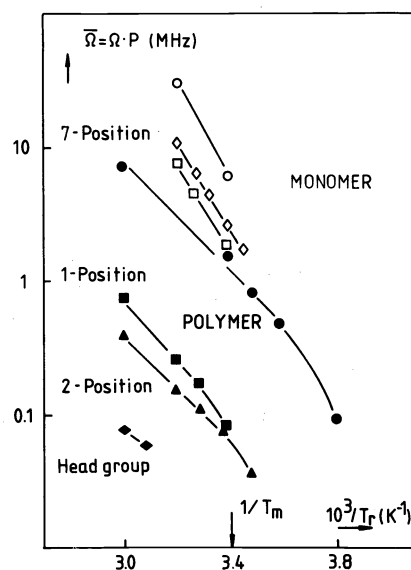


Fig. 17. Mean jump frequency  $\bar{\Omega}$  for the various positions in the monomer and polymer model membrane.

various methylene units of the lipid chain. The head group mobility is highly hindered by the polymerization well above the phase transition. The 6-site jump model described above can, therefore, be applied at the highest temperatures only. At lower temperatures only two site jumps indicative of interchange between two possible conformations only are observed.

This example shows again that highly selective information about molecular mobility can be obtained from  $^2\text{H}$  NMR. In this way we are able to show that by polymerizing a model membrane in its hydrophilic part a stable system can be generated which despite of motional hindrance in the head group region largely retains its chain flexibility most important for membrane applications.

**Acknowledgements:** I wish to thank all of my coworkers who have actively been engaged in the various experiments described in this survey. The fruitful cooperation with the research groups of Prof. H. Sillescu and Prof. H. Ringsdorf at the University of Mainz is also highly appreciated. The financial support of the Deutsche Forschungsgemeinschaft is gratefully acknowledged.

## REFERENCES

1. J.H. Wendorff and E.W. Fischer, Kolloid-Z. Z.Polym. **251**, 876 (1973).
2. W. Ruland and W. Wiegand, J. Polym. Sci. Polym.Symp. **58**, 43 (1977).
3. A.H. Windle in Developments in Oriented Polymers-1, edited by I.M. Ward Appl. Sci. Publ. London(1982).
4. T. Springer in Springer Tracts in Modern Physics Vol. 64 (1972).
5. J.S. Higgins, L.K. Nicholson and J.B. Hayter, Polymer **22**, 163 (1981).
6. F. Mezei (Ed.), Neutron Spin Echo, Springer-Verlag, Heidelberg (1980).
7. I.M. Ward (Ed.), Structure and Properties of Oriented Polymers, Appl. Sci. Publ. London (1975).
8. I.M. Ward (Ed.), Developments in Oriented Polymers-1, Appl. Sci. Publ., London (1982).
9. J.D. Ferry, Viscoelastic Properties of Polymers, J. Wiley, New York (1980).
10. R.T. Bailey, A.M. North, and R.A. Pethrick, Molecular Motion in High Polymers, Oxford Univ. Press, Oxford (1981).
11. H.H. Kausch and H.G. Zachmann (Eds.), Advances in Polymer Science, Vol. **66**, Springer-Verlag, Heidelberg (1985).
12. *ibid.* Vol. **67** (1985).
13. A. Abragam, The Principles of Nuclear Magnetism, Oxford Univ. Press, Oxford (1961).
14. H.W. Spiess, Colloid & Polymer Sci. **261**, 193 (1983).
15. H.W. Spiess in ref. 8, p. 47.
16. H.W. Spiess in ref. 11, p. 23.
17. J. Jeener and P. Broecker, Phys. Rev. **157**, 232 (1967).
18. H.W. Spiess and H. Sillescu, J. Magn. Resonance **42**, 381 (1980).
19. H.W. Spiess, J. Chem. Phys. **72**, 6755 (1980).
20. S. Wefing, S. Jurga and H.W. Spiess, Proc. XXIInd Congress Ampere, Zürich (1984) p. 375.
21. E. Rössler, H. Sillescu and H.W. Spiess, Polymer **26**, 203 (1985).
22. S. Wefing, F. Fajara, H. Sillescu and H.W. Spiess, to be published.
23. K.R. Jeffrey, Bull. Magn. Res. **3**, 69 (1981).
24. G. Williams and D.C. Watts, Trans. Faraday Soc. **66**, 80 (1970).
25. C.P. Lindsey and G.D. Patterson, J. Chem. Phys. **73**, 3348 (1970).
26. G.D. Patterson, Advances in Polymer Science **48**, 124 (1983).
27. V.C. McBrierty and D.C. Douglas, Phys. Rep. **63**, 61 (1980).
28. C. Schmidt, K.J. Kuhn and H.W. Spiess, submitted to Colloid & Polymer Science.
29. E.W. Fischer, G.P. Hellmann, H.W. Spiess, F.J. Hörth, U. Ecaris and M. Wehrle, Makromol. Chem., in press.
30. M. Gordon and N.A. Platé (Eds.), Advances in Polymer Science, Vols. 59-61 (1984).
31. L.L. Chapoy (Ed.), Recent Advances in Liquid Crystalline Polymers, Elsevier Appl. Sci. Publ., London (1985).
32. H. Finkelmann, H. Ringsdorf and J.H. Wendorff, Makromol. Chem. **179**, 273 (1978).
33. V.P. Shibaev, N.A. Platé and Y.S. Freidzon, J. Polym. Sci. Polym. Chem. Ed. **17**, 1655 (1979).
34. C. Boeffel, B. Hisgen, U. Pschorn, H. Ringsdorf and H.W. Spiess, Isr. J. Chem. **23**, 388 (1983).
35. H. Geib, B. Hisgen, U. Pschorn, H. Ringsdorf and H.W. Spiess, J. Am. Chem. Soc. **104**, 917 (1982).
36. R.G. Kirste and H.G. Ohm, Makromol. Chem. Rapid Commun. **6**, 179 (1985).
37. U. Pschorn, Ph.D. thesis, Univ. Mainz 1985.
38. R. Zentel, G.R. Strobl and H. Ringsdorf, Macromolecules, in press.
39. H. Bader, K. Dorn, B. Hupfer and H. Ringsdorf, Advances Polymer Science **64**, 1 (1985).
40. R. Ebelhäuser and H.W. Spiess, Makromol. Chem. Rapid Commun. **5**, 403 (1984).
41. R. Ebelhäuser and H.W. Spiess, Ber. Bunsenges. Phys. Chem., in press.